HHS Public Access

Author manuscript

ACS Chem Biol. Author manuscript; available in PMC 2024 August 16.

Published in final edited form as:

ACS Chem Biol. 2015 May 15; 10(5): 1160–1170. doi:10.1021/cb500923v.

Molecular Engineering of Nonmetallic Biosensors for CEST MRI

Amnon Bar-Shir[†,‡], **Jeff W. M. Bulte**[†,‡,§,∥,⊥,#], **Assaf A. Gilad**[*,†,‡,§]

[†]Russell H. Morgan Department of Radiology, The Johns Hopkins University School of Medicine, Baltimore, Maryland 21287, United States

[‡]Cellular Imaging Section and Vascular Biology Program, Institute for Cell Engineering, The Johns Hopkins University School of Medicine, Baltimore, Maryland 21205, United States

[§]F.M. Kirby Research Center for Functional Brain Imaging, Kennedy Krieger Institute, Baltimore, Maryland 21205, United States

[∥]Department of Biomedical Engineering, The Johns Hopkins University School of Medicine, Baltimore, Maryland 21205, United States

[⊥]Department of Chemical & Biomolecular Engineering, The Johns Hopkins University School of Medicine, Baltimore, Maryland 21218, United States

[#]Department of Oncology, The Johns Hopkins University School of Medicine, Baltimore, Maryland 21287, United States

Abstract

Recent advancements in molecular and synthetic biology, combined with synthetic chemistry and biotechnology, have opened up new opportunities to engineer novel platforms that can monitor complex biological processes with various noninvasive imaging modalities. After decades of using gadolinium- or iron-based metallic sensors for MRI, the recently developed chemical exchange saturation transfer (CEST) contrast mechanism has created an opportunity for rational design, *in silico*, of nonmetallic biosensors for MRI. These biomolecules are either naturally occurring compounds (amino acids, sugars, nucleosides, native proteins) or can be artificially engineered (synthetic probes or recombinant proteins). They can be administered either as exogenous agents or can be genetically (over)expressed. Moreover, they can be precisely engineered to achieve the desired biochemical properties for fine tuning optimized imaging schemes. The availability of these agents marks the dawn of a new scientific era for molecular and cellular MRI.

Graphical Abstract

[*]**Corresponding Author**: assaf.gilad@jhu.edu.

The authors declare the following competing financial interest(s): J.W.M.B. and A.A.G are co-owners of SenCEST, LLC.

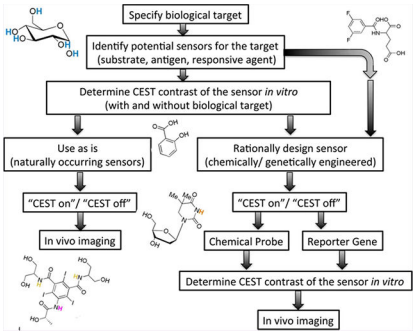

Understanding complex biological processes at the cellular level in live subjects is a key element in both basic science and clinical practice. Molecular and cellular imaging is a relatively new discipline that seeks to develop imaging toolboxes for the visualization, characterization, and quantification of (sub)cellular biologic processes. This can be accomplished using advanced imaging technologies, which include optical imaging, nuclear imaging, X-ray computed tomography (CT), ultrasound, and magnetic resonance imaging (MRI).[1–3] Synthetic imaging probes or genetically engineered imaging reporters have been developed for all of the aforementioned imaging modalities. These sensors are either biologically inert (to study location, a particular cell or organ, etc.) or biologically responsive (to study a process or function of interest). Among the imaging modalities, MRI is unique because longitudinal studies on a live subject can be performed, and the information obtained using biosensors or reporter genes can be coregistered with high-resolution anatomical images.

1. CEST MRI

In MRI, information is most commonly obtained by enhancing the contrast between the target and its surrounding tissue. This contrast can be enhanced by either manipulating the imaging acquisition parameters or by introducing chemical or biological entities also known as contrast agents (see Keywords). For many years, gadolinium (Gd^{3+})-based probes[4] and super-paramagnetic iron oxide (SPIO)-based particles[5] have been used to affect water relaxation properties (T_1 and T_2 or T_2*) and, consequently, the localized MR image contrast. Although Gd^{3+} agents have been used for the design of responsive MRI sensors, their metal origin might have adverse cellular effects that have not been elucidated yet in patients. The contrast generated by SPIO agents wipes out the ^{1}H MRI signal that is obtained from the imaged tissue, thus masking the anatomical information in the region of interest.

In 2000, a new contrast mechanism for MRI was proposed, termed chemical exchange saturation transfer (CEST).[6,7] In CEST MRI, a dynamic exchange process between an exchangeable proton and water protons is detected (Figure 1a; for a detailed review, see refs 8 and 9). By applying a radiofrequency (saturation) pulse at the resonance frequency (shifted by $\Delta\omega$ from the water protons) of the exchangeable pool of protons, the magnetization of this proton's pool is nullified (often referred to as saturated) and transferred to the bulk water protons through an exchange process. If the saturation pulse is applied for a sufficient time and the exchange process is fast enough (but still in the slow–intermediate exchange

regime on the NMR time scale), then an effect can be detected through the reduction of the water signal. This mechanism allows the detection of low-concentration CEST biosensors (from hundreds of micromolar to several millimolar) through the high ^{1}H MRI signal of the water. Although CEST contrast can be detected from endogenous components (e.g., glutamate,[10] creatine,[11] glycogen,[12] and others), it can be generated also by properly designed sensors. When combined with certain paramagnetic synthetic complexes, which induce highly shifted exchangeable protons (or water molecules), CEST can been termed PARACEST. PARACEST sensors were extensively studied, and their applications have been reviewed elsewhere;[8,13,14] however, since they are not based on natural compounds that are biodegradable, they are potentially toxic when not rapidly cleared from the body (as exemplified in the case of gadolinium). Most of the CEST MRI biosensors are based on proton exchange and detected through the changes in the water ^{1}H MRI signal. However, the CEST contrast that is based on two pools of exchangeable components, which have different chemical shift offsets ($\Delta\omega$) in NMR spectrum, was also recently extended to ^{19}F- and ^{129}Xe-based MRI (Figure 1b,c).[15,16] As both ^{19}F and ^{129}Xe nuclei do not exist in biological tissues, the information from heteronuclear-CEST (Hetero-CEST) can be overlaid on 1H MRI anatomical information and be presented as a hot-spot map.

2. RATIONALE FOR SELECTION AND DESIGN OF BIOSENSORS

The workflow in Figure 2 demonstrates the steps for CEST biosensor design toward a desired biological target. As a first step, a biological process or objective needs to be carefully specified. Such an objective may be, for example, a certain physiological condition (pH, temperature), an enzyme, a signaling or metabolic pathway, receptors, or a specific metal ion. In the next step, potential sensors (e.g., substrates, antigens, responsive agents) should be identified based on their putative CEST properties. It is important to determine the CEST contrast of the potential biosensor both before and after targeting the biological object (i.e., before and after enzymatic conversion, pH changes, etc.). It is essential to take into account that CEST contrast can be either turned on or off. A turn-on sensor may reflect a buildup of the contrast by changing proton exchange rates or by accumulation of the CEST probe. A turn-off sensor may reflect substrate conversion and elimination of the exchangeable proton.

Next, if a naturally occurring molecule that provides high contrast, high sensitivity, and high specificity can be identified, then *in vivo* imaging can be performed directly. Nevertheless, the sensor administration concentration and delivery method should be considered carefully (i.e., intravenously, (i.v.), intraperitoneal (i.p.), bolus or infusion, bare sensor, or embedded within a nanocarrier vehicle). Otherwise, if a naturally occurring probe does not exist or if CEST contrast is not satisfactory (e.g., poor contrast, small $\Delta\omega$, low sensitivity, and low specificity), then a molecular (synthetic or genetically) engineered CEST biosensor should be designed. By following a rational design for CEST biosensors, as reflected in the workflow depicted in Figure 2, both chemists and biologists will be able to generate new probes adapted specifically to their own research.

3. SMALL MOLECULES AS CEST BIOSENSORS

Small imaging probes are frequently used in a wide range of imaging modalities, including fluorescent or luminescent molecules for optical imaging, iodine-containing compounds for CT imaging, radioactive probes for positron emission tomography (PET) or single photon emission computed tomography (SPECT) applications, or contrast agents for MRI. The following section describes the use of small CEST biosensors for a range of applications from glucose uptake and metabolism imaging to real-time monitoring of gene expression. The depicted biosensors range from naturally occurring molecules (i.e., sugars, amino acids) to rationally designed synthetic molecules.

3.1. Imaging Glucose Uptake and Metabolism.

Primary and metastatic cancers are associated with upregulation of glycolysis, which results in increased levels of glucose uptake and consumption.[17] Moreover, overexpression of glucose transporters and glycolytic enzymes has been found in malignant tumors.[18] Therefore, monitoring glucose intake and metabolism in tumors has been a desired goal in cancer research for decades.[19] The glucose analogue 2-deoxy-D-glucose (2DG) cannot be metabolized further during glycolysis.[20] Hence, the radioactive tracer 2-[^{18}F]fluoro-2-deoxy-D-glucose (FDG),[21] which accumulates in tumor cells, has been the flagship agent of clinical PET applications for several decades.

Although glucose uptake and metabolism can be detected by MR spectroscopy (MRS)-based methodologies using ^{13}C-labeled glucose, which obviates the need for radioactive tracers, these methods suffer from low sensitivity and have poor-to-nonexistent spatial resolution.[19,20] Therefore, both the research groups of Golay and van Zijl capitalized on the five OH exchangeable protons of naturally occurring D-glucose (Figure 3a) to obtain spatial information from glucose uptake by tumors using CEST and have termed this methodology glucoCEST.[22,23] The glucoCEST contrast originates from saturating the glucose-exchangeable protons that resonate at a range of frequency offsets from the water resonance (Figure 3a; $\Delta\omega$ = 0.8–2.1 ppm[22] or $\Delta\omega$ = 1.2–2.9 ppm[23]). The systemic administration of D-glucose resulted in sufficient sensitivity for the detection of glucose accumulation in tumor-bearing mice.[22,23] These studies demonstrated the potential of using a naturally occurring MRI biosensor (D-glucose) for *in vivo* applications. However, since it is difficult to distinguish between the intra- and extracellular glucose and to account for downstream metabolism via the glycolitic pathway of the intracellular glucose, the contribution of each of these components to the CEST contrast is complex and not fully understood. The glucose analogue 2DG is phosphorylated to 2DG-6-phosphate (2DG6P) when taken up by cells, and it then accumulates in the cells since it cannot be furthered metabolized by the glycolytic pathway. Therefore, 2DG (Figure 3a) has been considered a turn-on CEST alternative for glucoCEST imaging[24,25] in the same manner as FDG is used for PET. Very recently, the using of 3-*O*-methyl-D-glucose (3OMG), a nontoxic and nonmetabolic derivative of glucose, was also used for CEST imaging of tumors.[26]

3.2. pH Sensing.

The acidity (pH) of intracellular compartments[27] in living cells plays a key role in many cellular processes, such as apoptosis, endocytosis, ion transport, and others. These events are studied mostly using fluorescent dyes[28] or genetically encoded fluorescent proteins engineered for pH sensing.[29] Since CEST contrast is affected dramatically by the exchange rate (k_{ex}) between the exchangeable protons and the water protons and the k_{ex} is dependent on pH,[8] it is feasible to map pH using CEST MRI. Therefore, theoretically, each CEST agent can be used to measure pH, as demonstrated for several probes in the original papers of Balaban and co-workers.[6,7] Chan et al. relied on the guanidine exchangeable protons of the amino acid L-arginine (Figure 3b; $\Delta\omega$ = 2.0 ppm) as a pH-sensitive CEST contrast agent for the noninvasive imaging of the viability of transplanted cells.[30] In this case, CEST contrast is turned off upon pH lowering as a consequence of cell death. To avoid dependency on the biosensor concentrations, compounds with more than one exchangeable proton pool, which resonates at a different $\Delta\omega$ and has a different exchange rate with water, were suggested as pH CEST sensors. One example is the amide protons of iopamidol (Figure 3b; $\Delta\omega_1$ = 4.2 ppm, $\Delta\omega_2$ = 5.5 ppm), which can be used in a ratiometric method for pH assessment.[31] Later, iobitridol, an analogue of iopamidol that contains a single set of amide protons, was used for *in vivo* pH mapping with CEST.[32]

One of the main obstacles of the aforementioned CEST biosensors is their relatively low $\Delta\omega$, which may result in (i) direct saturation of the water protons (during the saturation of the magnetization of the exchangeable proton) and (ii) contributions from endogenous CEST contrast (mostly from sugars, amino acids, peptides, and proteins). Moreover, CEST sensors with a relatively low $\Delta\omega$ may not be applicable for MRI scanners operating at low magnetic fields (especially 1.5–3.0 T clinical scanners, compared to the common 9.4–11.7 T preclinical scanners).[8] The hydroxyl proton of salicylic acid (Figure 3b) and its derivatives was suggested as a CEST contrast generator with highly shifted exchangeable protons ($\Delta\omega$ = 8.7–10.8 ppm), probably due to the intramolecular hydrogen bonding found in these molecules.[33] These probes, which demonstrate (so far) the largest $\Delta\omega$ between water protons and exchangeable protons for CEST agents, are pH-sensitive and can be monitored *in vivo*. Since these compounds can be easily chemically modified, they appear to be ideally suited for further development of CEST sensors.[34,35]

3.3. Monitoring Genetically Encoded Enzyme/Substrate Systems.

Monitoring enzyme activity longitudinally and noninvasively is crucial for many disciplines of the biomedical sciences. PET,[36] SPECT,[37] and bioluminescent imaging (BLI)[38,39] are well-established and highly sensitive modalities for imaging genetically encoded reporter systems. These reporter systems couple an efficient enzyme to a specific substrate (sensor) that can be sensitively imaged upon its conversion. However, some subjective and intrinsic limitations of these modalities restrict their widespread use or clinical translatability. The complexity of synthesis (requiring large investments in infrastructure including a cyclotron) and relatively short half-life times of radiolabeled compounds, in addition to a limited number of clinical scanners (~1:8 ratio of PET/MRI scanners in the US), restricts the application of nuclear imaging-based technologies. Optical-based imaging modalities are limited by tissue penetration of light and, consequently, are not applicable for imaging

deep tissues, large animals, or humans. Therefore, there is an increasing need for MRI-based genetically engineered reporter systems as an alternative. Since ^{1}H CEST contrast is generated by exchangeable protons of the molecule of interest, there is no need to attach a metallic imaging moiety to alter the contrast. Such an addition dramatically changes the structure of the desired substrate and may significantly affect the conversion rate by the target enzyme. The use of CEST-based reporter probes (substrates) for imaging reporter genes (enzymes) has opened a new avenue for the design and use of small (natural or synthetic) molecules as imaging probes for monitoring enzyme expression and activity.[40–43]

Cytosine deaminase (CDase) is an enzyme that catalyzes the conversion of cytosine to uracil (Figure 3c) and is expressed exclusively in bacteria and yeast. Given that CDase is absent in mammalian cells and since it can also catalyze the conversion of the prodrug 5-fluorocytosine (5FC) into the chemotherapeutic agent 5-fluorouracil (5FU), it was suggested for use as a therapeutic gene for cancer treatment.[44] Although CDase expression and activity (Figure 3c) were monitored *in vivo* using ^{19}F MRS,[45] no spatial information could be observed. Liu et al. used CEST MRI to monitor CDase activity with its native substrate cytosine or the pro-drug 5FC.[42] In that study, the CEST contrast derived from the NH_2 protons (Figure 3c, $\Delta\omega$ = 2.0–2.4 ppm) of cytosine or 5FC was eliminated upon its conversion to uracil or 5FU. This system is depicted in the right-hand section of the workflow (Figure 2) and demonstrates the utilization of both natural (cytosine) and synthetic (5FC) substrates as imaging probes. The bacterial enzyme carboxypeptidase G2 (CPG2) mediates the release of the C-terminal glutamate residue from a wide range of N-acylating moieties. Accordingly, CPG2 was suggested as a therapeutic gene that converts a nitrogen mustard pro-drug (CMDA, 4[(2-chloroethyl)(2-mesyloxyethyl)amino] benzoyl L-glutamic acid)) to an active drug (4[(2-chloroethyl)(2-mesyloxyethyl)-amino] benzoic acid), which is a potent DNA cross-linking agent.[46] The synthetic molecule, 3,5-difluorobenzoyl-L-glutamate (3,5-DFBGlu, Figure 3c), was suggested to be a CPG2 substrate whose conversion could be imaged with CEST. Due to the fact that 3,5-DFBGlu conversion releases glutamate, through which its exchangeable protons (Figure 3c, $\Delta\omega$ = 3.0 ppm) generate CEST contrast,[10] a turn-on CEST contrast is obtained upon CPG2 activity. In this case, the different k_{ex} (and, therefore, the CEST contrast) of amide (in 3,5-DFBGlu) and amine (in glutamate) functional groups was exploited to monitor CPG2 enzyme activity with CEST MRI.[43] Note that the resulted effect on CEST contrast upon changing k_{ex} can be predicted *in silico* using mathematically simulations,[47,48] which may be beneficial for screening larger arrays of potential CEST probes.

In order to maximize the CEST imaging capabilities of genetically encoded enzyme/substrate systems, the following requirements should be fulfilled: (i) sufficient CEST contrast, (ii) efficient conversion of the substrate by the target enzyme, and (iii) selectivity, meaning the substrate should be minimally converted by other endogenous enzymes. The herpes simplex virus type-1 thymidine kinase (HSV1-tk) is an enzyme that phosphorylates a wide range of nucleoside analogues, including radioactive modified nucleosides that are accumulated in HSV1-tk-expressing cells upon their phosphorylation. This mechanism of action has been used to monitor many biological targets, using PET or SPECT in preclinical studies and in patients.[49–54] The large chemical shift offsets of imino protons of nucleosides from water protons make them potential CEST biosensors. However, the relatively fast k_{ex}

of the imino protons of uridine and thymidine (k_{ex} = 3000–5000 s^{-1} $\Delta\omega$ = 6.2 ppm)[55,56] reduces their potential to be used as CEST sensors.

On the basis of the right-hand section of the rational design workflow (Figure 2), it is possible to transform thymidine into a CEST MRI reporter probe, which is a specific substrate for HSV1-tk but not for endogenous cellular kinases.[40,41] Hydro-genation of the thymidine double bond led to a reduction in the aromaticity of the product, dihydrothymidine (DHT), and to a dramatic increase in the pK_a of the imino proton as compared to thymidine. This resulted in a reduced k_{ex} and improved CEST characteristics (k_{ex} = 800–1700 s^{-1}, $\Delta\omega$ = 5.0 ppm). Importantly, the pK_a value of the exchangeable protons of the synthetic CEST probe can be predicted *in silico* prior its preparation, using computational software,[57,58] enabling the screening of large numbers of potent probes.[41] Although DHT generates high CEST contrast, the similarity of its structure to the native nucleoside thymidine leads to its phosphorylation by endogeneous kinases and therefore additional chemical modification is required to obtain further specificity to HSV1-tk. Therefore, the addition of a methyl group at the 5-position of DHT, which results in 5-methyl-dihydrothymidine (5-MDHT, Figure 3c), makes it a preferable CEST probe with high specificity to HSV1-tk and a negligible conversion by other cellular kinases. Accordingly, following i.v. administration, 5-MDHT accumulates only in HSV1-tk-expressing cells, thus enabling the differentiation of these cells from wild-type cells using CEST MRI.[40,41]

4. GENETICALLY ENCODED PROTEINS AS CEST BIOSENSORS

The advantage of using fluorescent proteins as reporter genes is that no substrate administration is required.[59] This eliminates challenges such as probe delivery, accessibility, and toxicity. In MRI, reporter genes have been developed based on overexpressing iron storage and transporting proteins, which affect the T_2 and T_2* water relaxation times.[60–62] Although ferritin has been used *in vivo* in a variety of biological applications,[60,61,63–65] it was shown that iron preloading of transfected, transplanted cells is important for a reliable imaging of cells *in vivo*.[66]

4.1. CEST Reporter Genes.

Positively charged polymers were suggested as potential CEST contrast agents in the early 2000s.[67] One such polymer, poly-L-lysine, generates exceptionally high CEST contrast when the saturation pulse is applied at the resonance frequency of its amide protons ($\Delta\omega$ = 3.6 ppm). An artificial protein consisting of 200 lysine residues (termed lysine-rich protein, LRP, Figure 4a), which was genetically engineered and expressed in cells, was therefore proposed as a new MRI reporter gene.[68] The applicability of LRP was recently demonstrated to be a valuable tool for direct monitoring of oncolytic virotherapy.[69] Subsequently, libraries of a variety of peptides were screened to identify optimal amino acids and peptide sequences for obtaining CEST contrast.[70,71] Among these sequences, arginine-rich peptides and proteins showed favorable CEST contrast originating from both their guanidine protons ($\Delta\omega$ = 1.8 ppm) and amide protons ($\Delta\omega$ = 3.6 ppm). The arginine-rich protein protamine from salmon, which consist of more than 60% arginine residues, showed a superior high

CEST contrast.[72] It was demonstrated that human protamine 1 (hPRM1, ~50% arginine, Figure 4b) can be used as a humanized CEST MRI reporter gene that allows differentiation between wild-type cells and cells that overexpress hPRM1.[73] One advantage of using genetically encoded systems is that libraries of biosensors can be generated using molecular biology tools (e.g., random mutagenesis and directed evolution), which can be used to select improved variants of the sensor.[74] However, efficient high-throughput screening, which is key for such an approach, should be carefully considered in order to allow the performance of this procedure within a manageable time scale. For example, for screening that relies on optical methods, an automated, confocal, real-time, and single-cell kinetic imaging system has been integrated into a single, compact unit.[75] Such a system will facilitate the screening and narrow it from millions of clones to a number of clones that can be scanned with MRI. Recently, lysine- and arginine-rich mutants of green fluorescent (GFP) proteins, aka supercharged GFP, showed increase in CEST contrast without compromising the fluorescent properties of the protein.[76] Thus, such reporters can be used as a template for high-throughput screening.

4.2. Responsive CEST Reporter Genes.

Protein kinases are enzymes that that play a key role in cellular signaling, with protein kinase A (PKA) being one of the most investigated ones. It is not surprising that many imaging sensors were therefore developed to monitor its activity, including the genetically encoded sensor for PKA regulation based on fluorescence resonance energy transfer (FRET).[77,78] Metal-loprotein-based sensors have also been developed to image PKA activity with MRI.[79]

As it is known that PKA phosphorylates the hydroxyl group (–OH) of serine (or threonine) with high specificity toward the peptide sequence LRRASLG,[80] the opportunity exists to image PKA activity with CEST MRI using a synthetic peptide (Figure 4c).[81] Interestingly, the CEST contrast obtained from the guanidine protons ($\Delta\omega$ = 1.8 ppm) and the amide protons ($\Delta\omega$ = 3.6 ppm) of the LRRASLG peptide was quenched upon its phosphorylation to LRRASpLG. Therefore, an artificial gene that encodes eight tandem repeats of the LRRASLG sequence was developed. This PKA biosensor, expressed in *Escherichia coli*, showed a higher CEST contrast compared to that of nontransfected controls. In this case, a turn-off CEST sensor was created to monitor cellular signaling. This concept can be expanded to other protein kinases as long as the phosphorylated sequence contains arginine and lysine residues that generate the CEST contrast and a phosphorylation site that allows conditional quenching of the signal.

5. HETERONUCLEAR (^{19}F AND ^{129}XE) CEST BIOSENSORS

One main intrinsic limitation of MRI contrast agents in general and of CEST agents in particular is the large concentration of water protons of the target tissue. Although the high proton concentration makes MRI a robust imaging methodology with a high signal-to-noise ratio (SNR), low concentrations of biosensors are less effective in altering the overall water ^{1}H MRI signal. Particularly for CEST contrast, submillimolar to several millimolar concentrations of the contrast agents are required for a detectable CEST

contrast.[8] Therefore, if the aim is to image a low-concentration target (e.g., metal ion levels or receptor of interest), then an alternative to ^{1}H CEST should be considered. Molecules with heteronuclear (i.e., other than ^{1}H) atoms, such as ^{3}He, ^{13}C, ^{15}N, ^{19}F, ^{31}P, and ^{129}Xe, have been suggested as sensors for MR-based applications due to the fact that their MR-active isotopes do not exist (or occur in negligible concentrations) in normal biological tissues.

Heteronuclear NMR experiments using saturation transfer modules were used to measure the exchange between two pools of (nonproton) nuclear spins[82–84] much earlier than reported in the original CEST MRI papers.[6,7] The combination of heteronuclear NMR and CEST opened a new avenue for the design of MRI sensors since it exploits the benefits of both methodologies, i.e., (i) the amplification effect of the CEST mechanism, and from the use of heteronuclear spins; (ii) the large chemical shifts (several hundreds of ppm for nonproton spins); (iii) the high sensitivity of the obtained $\Delta\omega$ to the local environment; and (iv) the lack of background signal. These advantages form the basis for the design and use of ^{19}F and ^{129}Xe CEST biosensors.

5.1. ^{19}F-CEST.

Metal ions play a crucial role in myriad biological processes, and the ability to monitor real-time changes in metal ion levels is essential for understanding a variety of physiological events. The design and use of fluorescent sensors to study variable changes in cellular levels of metal ions allows us to understand their role in cell biology.[85] Calcium (Ca^{2+}) signaling is used by all cell types to carry information and regulate various biochemical processes. In 1980, a new technology was developed that enabled the detection of intracellular levels of Ca^{2+} by using the synthetic fluorescent dye, 1,2-bis(*o*-aminophenoxy) ethane-*N,N,N,N*-tetraaceticacid (BAPTA).[86] This technology revolutionized our understanding of Ca^{2+} physiology and kindled the development of a variety of synthetic-[85] and genetic[87]-based calcium indicators. Although exciting advances in molecular biology now provide the opportunity to obtain long-term functional imaging of Ca^{2+} signaling *in vivo* via genetically encoded Ca^{2+} indicators based on fluorescent proteins,[88,89] the light source on which these methodologies are based is an obstacle with regard to deep tissue penetration and applicability for large animals and humans.

Interestingly, synthetic fluorinated derivatives of BAPTA showed a unique $\Delta\omega$ on the ^{19}F NMR spectrum and a different dissociation constant (K_d) between ion-bound and free F-BAPTA when fluorine was substituted at a different positions of the aminophenoxy ring (3-, 4-, 5-, or 6-position).[90,91] The 5F-BAPTA derivative was identified as a potential sensor for monitoring Ca^{2+} ions by combining ^{19}F MRI and CEST MRI, since the k_{ex} between Ca^{2+}-bound and free 5F-BAPTA was reported to be 150–550 s^{-1},[84,91] an optimal k_{ex} for a $\Delta\omega$ of ~6 ppm. In addition, the possibility of transferring magnetization between Ca^{2+}-bound and Ca^{2+}-free 5F-BAPTA during NMR experiments was demonstrated.[84] By performing a ^{19}F CEST MRI experiment, low concentrations (500 nM) of Ca^{2+} ions could be imaged with high specificity (compared to competing ions). This resulted from the unique $\Delta\omega$ (in the ^{19}F-NMR spectrum, Figure 5a) between free 5F-BAPTA and ion-bound 5F-BAPTA resonances for each ion (e.g., Ca^{2+}, Zn^{2+}, or Mg^{2+}), and the different k_{ex} between free and bound

5F-BAPTA for each examined ion. While Zn^{2+}-5F-BAPTA or Mg^{2+}-5F-BAPTA exchanged with free 5F-BAPTA too slow or too fast, respectively, to be detected by 19F CEST, the k_{ex} between Ca^{2+}-5F-BAPTA and free bulk 5F-BAPTA allows the transfer of saturation and thus Ca^{2+} detection.[15] This approach, termed ion CEST (iCEST), can be further extended and optimized to monitor different metal ions at variable levels by the rational design and synthesis of fluorinated ion chelates. One main advantage of the iCEST methodology is that the high specificity toward an ion of interest is reflected by two parameters, $\Delta\omega$ and k_{ex}, making this approach more ion specific. In an additional report, it was shown that further modification of 5F-BAPTA to obtained 5,5,6,6-tetrafluoro-BAPTA (TF-BAPTA) as the ^{19}F iCEST probe allows the detection of both Zn^{2+} and Fe^{2+} ions specifically and simultaneously and thus is termed multi-ion CEST (miCEST).[92] For novel probe design, such an approach eliminates the need to attach an imaging-responsive moiety to the binding chelate, as required for metal-based MRI sensors,[93,94] allowing a straightforward, rational synthetic design of ion sensors. Finally, the rising interest in ^{19}F MRI applications[95,96] as an alternative to (super)paramagnetic sensors[4,97] may lead to further use of ^{19}F-based MRI

5.2. Hyperpolarized ^{129}Xe-CEST.

Since hyperpolarized nuclear spins show a nearly 10^4-fold signal enhancement over nonpolarized elements, hyperpolarized-based approaches have the potential to significantly impact the field of molecular and cellular MR imaging. Hyperpolarized ^{13}C has been extensively studied and has already been translated to the clinic.[98] ^{129}Xe can also be hyperpolarized[99] and is an interesting nucleus for molecular and cellular MRI applications. In an elegant approach, the combination of hyperpolarized ^{129}Xe gas and CEST (Hyper-CEST) was demonstrated.[16,100] By exploiting the chemical shift difference between entrapped and free hyperpolarized ^{129}Xe gas, the potential of using Hyper-CEST for molecular and cellular imaging applications was shown (Figure 5b).

Cryptophanes are a group of molecular cages that can reversibly encapsulate a variety of guests, including halomethanes, ammonium salts, and noble gases, in particular Xe.[101] The ^{129}Xe NMR spectrum of the Xe–cryptophane complex in the presence of an excess of xenon shows two well-separated ($\Delta\omega$) signals at 229.5 and 62.3 ppm, which are assigned to free xenon in solution and to xenon trapped in the cryptohane cavity, respectively. Exploiting this $\Delta\omega$ and by binding a biotin-labeled cryptophane cage to avidin-functionalized agarose beads in an aqueous environment, an extremely low concentration of the biosensor (5 μM cryptophane) could be observed using HyperCEST.[16] The proof of concept of performing HyperCEST was recently established[102] and extended to monitor live cells that were loaded with fluorescently labeled cryptophanes.[103] Cryptophane-A was also used to tag antibodies for targeted detection of cellular antigen CD14.[104] In a different route, surfactant-stabilized perfluorocarbon-in-water nanoemulsions (Figure 5b) were suggested as molecular sensors for HyperCEST applications.[100] Taking advantage of the $\Delta\omega$ between the hyperpolarized ^{129}Xe at the aqueous solution and the interior of nanoemulsions and of the fact that ^{129}Xe freely exchanges between the two compartments, it was shown that the nanoemulsion can be detected at concentrations as low as 100 fM, corresponding to <1 μL of perfluorocarbon per liter of solution using HyperCEST. Due to the difference in the chemical shift of these two cages, it was possible to detect simultaneously two cell populations.[105] Finally,

genetically encoded gas nanovesicles from buoyant microbes were used as cages that entrap hyperpolarized Xe. These nanovesicles are based on gas-binding protein nanostructures expressed by certain buoyant microorganisms, which can be cloned and expressed in bacteria. However, since it is a cluster of genes, a proper expression in mammalian cells maybe challenging. These nanovesicles are different in size and therefore displayed maximal hyperCEST contrast at different saturation frequencies.[106] These new strategies for molecular-engineered nanosize HyperCEST sensors have the potential to be further explored and to be added to the HyperCEST toolbox for imaging molecular and cellular events.

6. ADDITIONAL TECHNICAL CONSIDERATIONS

It is important to note that when using high-power RF pulses in a CEST experiment a direct saturation of the MR frequency of the surrounding water molecules occurs. This is an impediment to using CEST probes with a relative small $\Delta\omega$ (0–2 ppm) and calls for the design and of CEST sensors having a larger $\Delta\omega$ of their exchangeable protons.[107] Furthermore, the use of strong RF pulses may lead to exceeding approved specific absorbance rates (SAR), which is a measure of the potential for RF-induced heating. This has to be taken into account when CEST experiments are being performed *in vivo*, especially in a clinical setup. To overcome these SAR limitations, the commonly used continuous wave (CW) RF irradiation cannot be used. Alternative schemes using short repeated RF irradiation pulses (pulsed-CEST imaging) may be considered.[108,109]

Although the absolute concentration of CEST sensors may be assessed quantitatively, many variables may limit an accurate quantification *in vivo*. This includes the unknown number and properties of other exchangeable pools present in the studied region and the T_2 exchange (T_{2ex}) effect.[110] Endogenous magnetization transfer may also complicate the determination of CEST sensor concentrations.[111] In addition, pH changes that affect the CEST signal magnitude also interfere with quantification. Finally, B_0 and B_1 inhomogeneities restrict the ability to determine the concentration of the CEST sensor solely from the obtained CEST contrast. While B_0 and B_1 inhomogeneities can be mapped[112,113] and corrected post data acquisition, the determination of the effect of the other abovementioned parameters on CEST amplitude (number of exchangeable pools, T_{2ex}, endogenous MT, and pH) is not straightforward. Therefore, if applicable, the acquisition of baseline CEST data prior to the CEST sensor administration is recommended, allowing the normalization of the CEST contrast relative to endogenous contributions.

7. CONCLUSIONS

In summary, in light of the recent demand for new tools that will allow better investigation of complex processes, a new field has evolved at the interfaces of synthetic chemistry, molecular engineering, and cellular imaging. It is now clear that it would be very difficult to find a single perfect agent for imaging all biological targets. Therefore, a better approach is to tailor the imaging probe or the sensor to perform a specific task. The rising field of CEST MRI offers chemists and biologists the opportunity to design large arrays of metal-free MRI sensors that can tackle particular questions. To that end, following the workflow described in Figure 2 may be beneficial for the development of a desired sensor.

After identifying the biological target, a potential sensor should be considered (natural or unnatural). If required, chemical modification or genetic manipulation of the sensor of interest should be performed based on a prediction (*in silico*, if applicable) of its properties. Screening of several optional probes may be performed prior to the selection of an optimal molecular probe that generates either CEST-off or CEST-on contrast for *in vitro* and *in vivo* applications. Following these steps may lead to the development of future nonmetallic biosensors for investigating complex biological questions.

ACKNOWLEDGMENTS

Supported by grants MSCRFII-0042, MSCRFF-0103-00, R01 NS079288, 2RO1 NS045062, and R21 EB005252. The authors would like to thank Ms. M. McAllister for her assistance in editing the manuscript.

KEYWORDS

(Bio)sensor
an imaging agent used to monitor a biological phenomenon or target

Contrast agent
An imaging probe that changes the target signal in the image relative to the background signal, creating contrast

Small molecule biosensor
Nonpolymeric chemical substance with low molecular weight, e.g., sugar, amino acid, nucleoside, or other naturally occurring or synthetic compound

Genetically engineered enzyme/substrate reporter system
A system that consists of two components, (i) a recombinant enzyme and (ii) its substrate, which allows imaging of enzyme expression and/or activity

Reporter gene
A gene whose product acts as a beacon for a certain imaging modality

Responsive reporter gene
A reporter gene that changes its imaging properties (enhances signal, changes color, etc.) upon a change in biological events (i.e., enzymatic activity, ion levels, regulation of cellular function)

CEST
Chemical exchange saturation transfer

HeteroCEST
CEST experiments that do not involve protons (e.g., ^{19}F or ^{129}Xe)

iCEST
Ion CEST. A methodology that enables the detection of metal ions using their fluorinated chelate when performing ^{19}F CEST MRI

HyperCEST

Hyperpolarized CEST. A methodology developed for molecular imaging applications using hyperpolarized ^{129}Xe gas as the imaging agent

REFERENCES

(1). Willmann JK, van Bruggen N, Dinkelborg LM, and Gambhir SS (2008) Molecular imaging in drug development. Nat. Rev. Drug Discovery 7, 591–607. [PubMed: 18591980]

(2). Betzer O, Shwartz A, Motiei M, Kazimirsky G, Gispan I, Damti E, Brodie C, Yadid G, and Popovtzer R (2014) Nanoparticle-based CT imaging technique for longitudinal and quantitative stem cell tracking within the brain: application in neuropsychiatric disorders. ACS Nano 8, 9274–9285. [PubMed: 25133802]

(3). Choi J, Park H, Kim T, Jeong Y, Oh MH, Hyeon T, Gilad AA, and Lee KH (2014) Engineered collagen hydrogels for the sustained release of biomolecules and imaging agents: promoting the growth of human gingival cells. Int. J. Nanomed 9, 5189–5201.

(4). Caravan P (2006) Strategies for increasing the sensitivity of gadolinium based MRI contrast agents. Chem. Soc. Rev 35, 512–523. [PubMed: 16729145]

(5). Bulte JW, and Kraitchman DL (2004) Iron oxide MR contrast agents for molecular and cellular imaging. NMR Biomed. 17, 484–499. [PubMed: 15526347]

(6). Ward KM, Aletras AH, and Balaban RS (2000) A new class of contrast agents for MRI based on proton chemical exchange dependent saturation transfer (CEST). J. Magn. Reson 143, 79–87. [PubMed: 10698648]

(7). Ward KM, and Balaban RS (2000) Determination of pH using water protons and chemical exchange dependent saturation transfer (CEST). Magn. Reson. Med 44, 799–802. [PubMed: 11064415]

(8). van Zijl PC, and Yadav NN (2011) Chemical exchange saturation transfer (CEST): what is in a name and what isn't? Magn. Reson. Med 65, 927–948. [PubMed: 21337419]

(9). Tsitovich PB, Burns PJ, McKay AM, and Morrow JR (2014) Redox-activated MRI contrast agents based on lanthanide and transition metal ions. J. Inorg. Biochem 133, 143–154. [PubMed: 24529651]

(10). Cai K, Haris M, Singh A, Kogan F, Greenberg JH, Hariharan H, Detre JA, and Reddy R (2012) Magnetic resonance imaging of glutamate. Nat. Med 18, 302–306. [PubMed: 22270722]

(11). Haris M, Singh A, Cai K, Kogan F, McGarvey J, Debrosse C, Zsido GA, Witschey WR, Koomalsingh K, Pilla JJ, Chirinos JA, Ferrari VA, Gorman JH, Hariharan H, Gorman RC, and Reddy R (2014) A technique for in vivo mapping of myocardial creatine kinase metabolism. Nat. Med 20, 209–214. [PubMed: 24412924]

(12). van Zijl PC, Jones CK, Ren J, Malloy CR, and Sherry AD (2007) MRI detection of glycogen in vivo by using chemical exchange saturation transfer imaging (glycoCEST). Proc. Natl. Acad. Sci. U.S.A 104, 4359–4364. [PubMed: 17360529]

(13). Viswanathan S, Kovacs Z, Green KN, Ratnakar SJ, and Sherry AD (2010) Alternatives to gadolinium-based metal chelates for magnetic resonance imaging. Chem. Rev 110, 2960–3018. [PubMed: 20397688]

(14). Terreno E, Castelli DD, and Aime S (2010) Encoding the frequency dependence in MRI contrast media: the emerging class of CEST agents. Contrast Media Mol. Imaging 5, 78–98. [PubMed: 20419761]

(15). Bar-Shir A, Gilad AA, Chan KW, Liu G, van Zijl PC, Bulte JW, and McMahon MT (2013) Metal ion sensing using ion chemical exchange saturation transfer ^{19}F magnetic resonance imaging. J. Am. Chem. Soc 135, 12164–12167. [PubMed: 23905693]

(16). Schroder L, Lowery TJ, Hilty C, Wemmer DE, and Pines A (2006) Molecular imaging using a targeted magnetic resonance hyperpolarized biosensor. Science 314, 446–449. [PubMed: 17053143]

(17). Gatenby RA, and Gillies RJ (2004) Why do cancers have high aerobic glycolysis? Nat. Rev. Cancer 4, 891–899. [PubMed: 15516961]

(18). Kim JW, and Dang CV (2006) Cancer's molecular sweet tooth and the Warburg effect. Cancer Res. 66, 8927–8930. [PubMed: 16982728]

(19). Plathow C, and Weber WA (2008) Tumor cell metabolism imaging. J. Nucl. Med 49, 43S–63S. [PubMed: 18523065]

(20). Woodward GE, and Hudson MT (1954) The effect of 2-desoxy-D-glucose on glycolysis and respiration of tumor and normal tissues. Cancer Res. 14, 599–605. [PubMed: 13199805]

(21). Ido T, Wan C-N, Casella V, Fowler JS, Wolf AP, Reivich M, and Kuhl DE (1978) Labeled 2-deoxy-D-glucose analogs. ^{18}F-labeled 2-deoxy-2-fluoro-D-glucose, 2-deoxy-2-fluoro-D-mannose and ^{14}C-2-deoxy-2-fluoro-D-glucose. J. Labelled Compd. Radiopharm 14, 175–183.

(22). Chan KW, McMahon MT, Kato Y, Liu G, Bulte JW, Bhujwalla ZM, Artemov D, and van Zijl PC (2012) Natural D-glucose as a biodegradable MRI contrast agent for detecting cancer. Magn. Reson. Med 68, 1764–1773. [PubMed: 23074027]

(23). Walker-Samuel S, Ramasawmy R, Torrealdea F, Rega M, Rajkumar V, Johnson SP, Richardson S, Goncalves M, Parkes HG, Arstad E, Thomas DL, Pedley RB, Lythgoe MF, and Golay X (2013) In vivo imaging of glucose uptake and metabolism in tumors. Nat. Med 19, 1067–1072. [PubMed: 23832090]

(24). Nasrallah FA, Pages G, Kuchel PW, Golay X, and Chuang KH (2013) Imaging brain deoxyglucose uptake and metabolism by glucoCEST MRI. J. Cereb. Blood Flow Metab 33, 1270–1278. [PubMed: 23673434]

(25). Rivlin M, Horev J, Tsarfaty I, and Navon G (2013) Molecular imaging of tumors and metastases using chemical exchange saturation transfer (CEST) MRI. Sci. Rep 3, 3045. [PubMed: 24157711]

(26). Rivlin M, Tsarfaty I, and Navon G (2014) Functional molecular imaging of tumors by chemical exchange saturation transfer MRI of 3-*O*-methyl-D-glucose. Magn. Reson. Med 72, 1375–1380. [PubMed: 25236979]

(27). Anderson RG, and Orci L (1988) A view of acidic intracellular compartments. J. Cell Biol 106, 539–543. [PubMed: 3279044]

(28). Han J, and Burgess K (2010) Fluorescent indicators for intracellular pH. Chem. Rev 110, 2709–2728. [PubMed: 19831417]

(29). Miesenbock G, De Angelis DA, and Rothman JE (1998) Visualizing secretion and synaptic transmission with pH-sensitive green fluorescent proteins. Nature 394, 192–195. [PubMed: 9671304]

(30). Chan KW, Liu G, Song X, Kim H, Yu T, Arifin DR, Gilad AA, Hanes J, Walczak P, van Zijl PC, Bulte JW, and McMahon MT (2013) MRI-detectable pH nanosensors incorporated into hydrogels for in vivo sensing of transplanted-cell viability. Nat. Mater 12, 268–275. [PubMed: 23353626]

(31). Longo DL, Dastru W, Digilio G, Keupp J, Langereis S, Lanzardo S, Prestigio S, Steinbach O, Terreno E, Uggeri F, and Aime S (2011) Iopamidol as a responsive MRI-chemical exchange saturation transfer contrast agent for pH mapping of kidneys: In vivo studies in mice at 7 T. Magn. Reson. Med 65, 202–211. [PubMed: 20949634]

(32). Longo DL, Sun PZ, Consolino L, Michelotti FC, Uggeri F, and Aime S (2014) A general MRI-CEST ratiometric approach for pH imaging: demonstration of in vivo pH mapping with iobitridol. J. Am. Chem. Soc 136, 14333–14336. [PubMed: 25238643]

(33). Yang X, Song X, Li Y, Liu G, Ray Banerjee S, Pomper MG, and McMahon MT (2013) Salicylic acid and analogues as diaCEST MRI contrast agents with highly shifted exchangeable proton frequencies. Angew. Chem., Int. Ed 52, 8116–8119.

(34). Song X, Yang X, Ray Banerjee S, Pomper MG, and McMahon MT (2014) Anthranilic acid analogs as diamagnetic CEST MRI contrast agents that feature an intramolecular-bond shifted hydrogen. Contrast Media Mol. Imaging 10, 74–80. [PubMed: 24771546]

(35). Yang X, Yadav NN, Song X, Ray Banerjee S, Edelman H, Minn I, van Zijl PC, Pomper MG, and McMahon MT (2014) Tuning phenols with intra-molecular bond shifted hydrogens (IM-SHY) as diaCEST MRI contrast agents. Chemistry 20, 15824–15832. [PubMed: 25302635]

(36). Gambhir SS, Bauer E, Black ME, Liang Q, Kokoris MS, Barrio JR, Iyer M, Namavari M, Phelps ME, and Herschman HR (2000) A mutant herpes simplex virus type 1 thymidine kinase reporter

gene shows improved sensitivity for imaging reporter gene expression with positron emission tomography. Proc. Natl. Acad. Sci. U.S.A 97, 2785–2790. [PubMed: 10716999]

(37). Tjuvajev JG, Finn R, Watanabe K, Joshi R, Oku T, Kennedy J, Beattie B, Koutcher J, Larson S, and Blasberg RG (1996) Noninvasive imaging of herpes virus thymidine kinase gene transfer and expression: a potential method for monitoring clinical gene therapy. Cancer Res. 56, 4087–4095. [PubMed: 8797571]

(38). Thompson EM, Adenot P, Tsuji FI, and Renard JP (1995) Real time imaging of transcriptional activity in live mouse preimplantation embryos using a secreted luciferase. Proc. Natl. Acad. Sci. U.S.A 92, 1317–1321. [PubMed: 7877974]

(39). Prescher JA, and Contag CH (2010) Guided by the light: visualizing biomolecular processes in living animals with bioluminescence. Curr. Opin. Chem. Biol 14, 80–89. [PubMed: 19962933]

(40). Bar-Shir A, Liu G, Greenberg MM, Bulte JW, and Gilad AA (2013) Synthesis of a probe for monitoring HSV1-tk reporter gene expression using chemical exchange saturation transfer MRI. Nat. Protoc 8, 2380–2391. [PubMed: 24177294]

(41). Bar-Shir A, Liu G, Liang Y, Yadav NN, McMahon MT, Walczak P, Nimmagadda S, Pomper MG, Tallman KA, Greenberg MM, van Zijl PC, Bulte JW, and Gilad AA (2013) Transforming thymidine into a magnetic resonance imaging probe for monitoring gene expression. J. Am. Chem. Soc 135, 1617–1624. [PubMed: 23289583]

(42). Liu G, Liang Y, Bar-Shir A, Chan KW, Galpoththawela CS, Bernard SM, Tse T, Yadav NN, Walczak P, McMahon MT, Bulte JW, van Zijl PC, and Gilad AA (2011) Monitoring enzyme activity using a diamagnetic chemical exchange saturation transfer magnetic resonance imaging contrast agent. J. Am. Chem. Soc 133, 16326–16329. [PubMed: 21919523]

(43). Jamin Y, Eykyn TR, Poon E, Springer CJ, and Robinson SP (2013) Detection of the prodrug-activating enzyme carboxypeptidase G2 activity with chemical exchange saturation transfer magnetic resonance. Mol. Imaging Biol 16, 152–157.

(44). Huber BE, Austin EA, Richards CA, Davis ST, and Good SS (1994) Metabolism of 5-fluorocytosine to 5-fluorouracil in human colorectal tumor cells transduced with the cytosine deaminase gene: significant antitumor effects when only a small percentage of tumor cells express cytosine deaminase. Proc. Natl. Acad. Sci. U.S.A 91, 8302–8306. [PubMed: 8058798]

(45). Stegman LD, Rehemtulla A, Beattie B, Kievit E, Lawrence TS, Blasberg RG, Tjuvajev JG, and Ross BD (1999) Noninvasive quantitation of cytosine deaminase transgene expression in human tumor xenografts with in vivo magnetic resonance spectroscopy. Proc. Natl. Acad. Sci. U.S.A 96, 9821–9826. [PubMed: 10449778]

(46). Hedley D, Ogilvie L, and Springer C (2007) Carboxypeptidase-G2-based gene-directed enzyme-prodrug therapy: a new weapon in the GDEPT armoury. Nat. Rev. Cancer 7, 870–879. [PubMed: 17943135]

(47). Woessner DE, Zhang S, Merritt ME, and Sherry AD (2005) Numerical solution of the Bloch equations provides insights into the optimum design of PARACEST agents for MRI. Magn. Reson. Med 53, 790–799. [PubMed: 15799055]

(48). McMahon MT, Gilad AA, Zhou J, Sun PZ, Bulte JW, and van Zijl PC (2006) Quantifying exchange rates in chemical exchange saturation transfer agents using the saturation time and saturation power dependencies of the magnetization transfer effect on the magnetic resonance imaging signal (QUEST and QUESP): pH calibration for poly-L-lysine and a starburst dendrimer. Magn. Reson. Med 55, 836–847. [PubMed: 16506187]

(49). Cao F, Lin S, Xie X, Ray P, Patel M, Zhang X, Drukker M, Dylla SJ, Connolly AJ, Chen X, Weissman IL, Gambhir SS, and Wu JC (2006) In vivo visualization of embryonic stem cell survival, proliferation, and migration after cardiac delivery. Circulation 113, 1005–1014. [PubMed: 16476845]

(50). Koehne G, Doubrovin M, Doubrovina E, Zanzonico P, Gallardo HF, Ivanova A, Balatoni J, Teruya-Feldstein J, Heller G, May C, Ponomarev V, Ruan S, Finn R, Blasberg RG, Bornmann W, Riviere I, Sadelain M, O'Reilly RJ, Larson SM, and Tjuvajev JG (2003) Serial in vivo imaging of the targeted migration of human HSV-TK-transduced antigen-specific lymphocytes. Nat. Biotechnol 21, 405–413. [PubMed: 12652311]

(51). Yaghoubi SS, and Gambhir SS (2006) PET imaging of herpes simplex virus type 1 thymidine kinase (HSV1-tk) or mutant HSV1-sr39tk reporter gene expression in mice and humans using [^{18}F]FHBG. Nat. Protoc 1, 3069–3075. [PubMed: 17406570]

(52). Wu JC, Cao F, Dutta S, Xie X, Kim E, Chungfat N, Gambhir S, Mathewson S, Connolly AJ, Brown M, and Wang EW (2006) Proteomic analysis of reporter genes for molecular imaging of transplanted embryonic stem cells. Proteomics 6, 6234–6249. [PubMed: 17080479]

(53). Wu JC, Chen IY, Sundaresan G, Min JJ, De A, Qiao JH, Fishbein MC, and Gambhir SS (2003) Molecular imaging of cardiac cell transplantation in living animals using optical bioluminescence and positron emission tomography. Circulation 108, 1302–1305. [PubMed: 12963637]

(54). Yaghoubi SS, Jensen MC, Satyamurthy N, Budhiraja S, Paik D, Czernin J, and Gambhir SS (2009) Noninvasive detection of therapeutic cytolytic T cells with 18F-FHBG PET in a patient with glioma. Nat. Clin. Pract. Oncol 6, 53–58. [PubMed: 19015650]

(55). Snoussi K, Bulte JW, Gueron M, and van Zijl PC (2003) Sensitive CEST agents based on nucleic acid imino proton exchange: detection of poly(rU) and of a dendrimer-poly(rU) model for nucleic acid delivery and pharmacology. Magn. Reson. Med 49, 998–1005. [PubMed: 12768576]

(56). Yadav NN, Jones CK, Xu J, Bar-Shir A, Gilad AA, McMahon MT, and van Zijl PC (2012) Detection of rapidly exchanging compounds using on-resonance frequency-labeled exchange (FLEX) transfer. Magn. Reson. Med 68, 1048–1055. [PubMed: 22837066]

(57). Milletti F, Storchi L, Goracci L, Bendels S, Wagner B, Kansy M, and Cruciani G (2010) Extending pKa prediction accuracy: high-throughput pKa measurements to understand pKa modulation of new chemical series. Eur. J. Med. Chem 45, 4270–4279. [PubMed: 20633962]

(58). Manchester J, Walkup G, Rivin O, and You Z (2010) Evaluation of pKa estimation methods on 211 druglike compounds. J. Chem. Inf. Model 50, 565–571. [PubMed: 20225863]

(59). Tsien RY (2009) Constructing and exploiting the fluorescent protein paintbox (Nobel Lecture). Angew. Chem., Int. Ed 48, 5612–5626.

(60). Genove G, DeMarco U, Xu H, Goins WF, and Ahrens ET (2005) A new transgene reporter for in vivo magnetic resonance imaging. Nat. Med 11, 450–454. [PubMed: 15778721]

(61). Cohen B, Ziv K, Plaks V, Israely T, Kalchenko V, Harmelin A, Benjamin LE, and Neeman M (2007) MRI detection of transcriptional regulation of gene expression in transgenic mice. Nat. Med 13, 498–503. [PubMed: 17351627]

(62). Zurkiya O, Chan AW, and Hu X (2008) MagA is sufficient for producing magnetic nanoparticles in mammalian cells, making it an MRI reporter. Magn. Reson. Med 59, 1225–1231. [PubMed: 18506784]

(63). Cohen B, Dafni H, Meir G, Harmelin A, and Neeman M (2005) Ferritin as an endogenous MRI reporter for noninvasive imaging of gene expression in C6 glioma tumors. Neoplasia 7, 109–117. [PubMed: 15802016]

(64). Iordanova B, and Ahrens ET (2012) In vivo magnetic resonance imaging of ferritin-based reporter visualizes native neuroblast migration. NeuroImage 59, 1004–1012. [PubMed: 21939774]

(65). Kim HS, Cho HR, Choi SH, Woo JS, and Moon WK (2010) In vivo imaging of tumor transduced with bimodal lentiviral vector encoding human ferritin and green fluorescent protein on a 1.5T clinical magnetic resonance scanner. Cancer Res. 70, 7315–7324. [PubMed: 20823165]

(66). Vandsburger MH, Radoul M, Addadi Y, Mpofu S, Cohen B, Eilam R, and Neeman M (2013) Ovarian carcinoma: quantitative biexponential MR imaging relaxometry reveals the dynamic recruitment of ferritin-expressing fibroblasts to the angiogenic rim of tumors. Radiology 268, 790–801. [PubMed: 23801774]

(67). Goffeney N, Bulte JW, Duyn J, Bryant LH Jr., and van Zijl PC (2001) Sensitive NMR detection of cationic-polymer-based gene delivery systems using saturation transfer via proton exchange. J. Am. Chem. Soc 123, 8628–8629. [PubMed: 11525684]

(68). Gilad AA, McMahon MT, Walczak P, Winnard PT Jr., Raman V, van Laarhoven HW, Skoglund CM, Bulte JW, and van Zijl PC (2007) Artificial reporter gene providing MRI contrast based on proton exchange. Nat. Biotechnol 25, 217–219. [PubMed: 17259977]

(69). Farrar CT, Buhrman JS, Liu G, Kleijn A, Lamfers ML, McMahon MT, Gilad AA, and Fulci G (2015) Establishing the lysine-rich protein CEST reporter gene as a CEST MR imaging detector for oncolytic virotherapy. Radiology, 140251.

(70). McMahon MT, Gilad AA, DeLiso MA, Berman SM, Bulte JW, and van Zijl PC (2008) New "multicolor" polypeptide diamagnetic chemical exchange saturation transfer (DIACEST) contrast agents for MRI. Magn. Reson. Med 60, 803–812. [PubMed: 18816830]

(71). Liu G, Gilad AA, Bulte JW, van Zijl PC, and McMahon MT (2010) High-throughput screening of chemical exchange saturation transfer MR contrast agents. Contrast Media Mol. Imaging 5, 162–170. [PubMed: 20586030]

(72). Choi J, Kim K, Kim T, Liu G, Bar-Shir A, Hyeon T, McMahon MT, Bulte JW, Fisher JP, and Gilad AA (2011) Multimodal imaging of sustained drug release from 3-D poly-(propylene fumarate) (PPF) scaffolds. J. Controlled Release 156, 239–245.

(73). Bar-Shir A, Liu G, Chan KW, Oskolkov N, Song X, Yadav NN, Walczak P, McMahon MT, van Zijl PC, Bulte JW, and Gilad AA (2014) Human protamine-1 as an MRI reporter gene based on chemical exchange. ACS Chem. Biol 9, 134–138. [PubMed: 24138139]

(74). Shapiro MG, Westmeyer GG, Romero PA, Szablowski JO, Kuster B, Shah A, Otey CR, Langer R, Arnold FH, and Jasanoff A (2010) Directed evolution of a magnetic resonance imaging contrast agent for noninvasive imaging of dopamine. Nat. Biotechnol 28, 264–270. [PubMed: 20190737]

(75). Chan GK, Richards GR, Peters M, and Simpson PB (2005) High content kinetic assays of neuronal signaling implemented on BD pathway HT. Assay Drug Dev. Technol 3, 623–636. [PubMed: 16438658]

(76). Bar-Shir A, Liang Y, Chan KWY, Gilad AA, and Bulte JWM (2015) Supercharged green fluorescent proteins as bimodal reporter genes for CEST MRI and optical imaging. Chem. Commun 51, 4869–4871.

(77). Zhang J, Ma Y, Taylor SS, and Tsien RY (2001) Genetically encoded reporters of protein kinase A activity reveal impact of substrate tethering. Proc. Natl. Acad. Sci. U.S.A 98, 14997–15002. [PubMed: 11752448]

(78). Ni Q, Ganesan A, Aye-Han NN, Gao X, Allen MD, Levchenko A, and Zhang J (2011) Signaling diversity of PKA achieved via a Ca^{2+}–cAMP–PKA oscillatory circuit. Nat. Chem. Biol 7, 34–40. [PubMed: 21102470]

(79). Shapiro MG, Szablowski JO, Langer R, and Jasanoff A (2009) Protein nanoparticles engineered to sense kinase activity in MRI. J. Am. Chem. Soc 131, 2484–2486. [PubMed: 19199639]

(80). Kemp BE, Graves DJ, Benjamini E, and Krebs EG (1977) Role of multiple basic residues in determining the substrate specificity of cyclic AMP-dependent protein kinase. J. Biol. Chem 252, 4888–4894. [PubMed: 194899]

(81). Airan RD, Bar-Shir A, Liu G, Pelled G, McMahon MT, van Zijl PC, Bulte JW, and Gilad AA (2012) MRI biosensor for protein kinase A encoded by a single synthetic gene. Magn. Reson. Med 68, 1919–1923. [PubMed: 23023588]

(82). Kupriyanov VV, Balaban RS, Lyulina NV, Steinschneider A, and Saks VA (1990) Combination of ^{31}P-NMR magnetization transfer and radioisotope exchange methods for assessment of an enzyme reaction mechanism: rate-determining steps of the creatine kinase reaction. Biochim. Biophys. Acta 1020, 290–304. [PubMed: 2248962]

(83). Alger JR, and Shulman RG (1984) NMR studies of enzymatic rates in vitro and in vivo by magnetization transfer. Q. Rev. Biophys 17, 83–124. [PubMed: 6091170]

(84). Gilboa H, Chapman BE, and Kuchel PW (1994) ^{19}F NMR magnetization transfer between 5-FBAPTA and its complexes. An alternative means for measuring free Ca^{2+} concentration, and detection of complexes with protein in erythrocytes. NMR Biomed. 7, 330–338. [PubMed: 7718434]

(85). Domaille DW, Que EL, and Chang CJ (2008) Synthetic fluorescent sensors for studying the cell biology of metals. Nat. Chem. Biol 4, 168–175. [PubMed: 18277978]

(86). Tsien RY (1980) New calcium indicators and buffers with high selectivity against magnesium and protons: design, synthesis, and properties of prototype structures. Biochemistry 19, 2396–2404. [PubMed: 6770893]

(87). Miyawaki A, Llopis J, Heim R, McCaffery JM, Adams JA, Ikura M, and Tsien RY (1997) Fluorescent indicators for Ca^{2+} based on green fluorescent proteins and calmodulin. Nature 388, 882–887. [PubMed: 9278050]

(88). Wallace DJ, Meyer zum Alten Borgloh S, Astori S, Yang Y, Bausen M, Kugler S, Palmer AE, Tsien RY, Sprengel R, Kerr JN, Denk W, and Hasan MT (2008) Single-spike detection in vitro and in vivo with a genetic Ca^{2+} sensor. Nat. Methods 5, 797–804. [PubMed: 19160514]

(89). Pologruto TA, Yasuda R, and Svoboda K (2004) Monitoring neural activity and [Ca^{2+}] with genetically encoded Ca^{2+} indicators. J. Neurosci 24, 9572–9579. [PubMed: 15509744]

(90). Clarke SD, Metcalfe JC, and Smith GA (1993) Design and properties of new F-19 NMR Ca^{2+} indicators—modulation of the affinities of BAPTA derivatives via alkylation. J. Chem. Soc., Perkin Trans 2, 1187–1194.

(91). Smith GA, Hesketh RT, Metcalfe JC, Feeney J, and Morris PG (1983) Intracellular calcium measurements by ^{19}F NMR of fluorine-labeled chelators. Proc. Natl. Acad. Sci. U.S.A 80, 7178–7182. [PubMed: 6417665]

(92). Bar-Shir A, Yadav NN, Gilad AA, van Zijl PC, McMahon MT, and Bulte JW (2015) Single ^{19}F probe for simultaneous detection of multiple metal ions using miCEST MRI. J. Am. Chem. Soc 137, 78–81. [PubMed: 25523816]

(93). Atanasijevic T, Shusteff M, Fam P, and Jasanoff A (2006) Calcium-sensitive MRI contrast agents based on superparamagnetic iron oxide nanoparticles and calmodulin. Proc. Natl. Acad. Sci. U.S.A 103, 14707–14712. [PubMed: 17003117]

(94). Esqueda AC, Lopez JA, Andreu-de-Riquer G, Alvarado-Monzon JC, Ratnakar J, Lubag AJ, Sherry AD, and De Leon-Rodriguez LM (2009) A new gadolinium-based MRI zinc sensor. J. Am. Chem. Soc 131, 11387–11391. [PubMed: 19630391]

(95). Ruiz-Cabello J, Barnett BP, Bottomley PA, and Bulte JW (2011) Fluorine ^{19}F MRS and MRI in biomedicine. NMR Biomed. 24, 114–129. [PubMed: 20842758]

(96). Ahrens ET, and Bulte JW (2013) Tracking immune cells in vivo using magnetic resonance imaging. Nat. Rev. Immunol 13, 755–763. [PubMed: 24013185]

(97). Bulte JW (2005) Hot spot MRI emerges from the background. Nat. Biotechnol 23, 945–946. [PubMed: 16082363]

(98). Nelson SJ, Kurhanewicz J, Vigneron DB, Larson PE, Harzstark AL, Ferrone M, van Criekinge M, Chang JW, Bok R, Park I, Reed G, Carvajal L, Small EJ, Munster P, Weinberg VK, Ardenkjaer-Larsen JH, Chen AP, Hurd RE, Odegardstuen LI, Robb FJ, Tropp J, and Murray JA (2013) Metabolic imaging of patients with prostate cancer using hyperpolarized [1-^{13}C]pyruvate. Sci. Transl. Med 5, 198ra108.

(99). Navon G, Song YQ, Room T, Appelt S, Taylor RE, and Pines A (1996) Enhancement of solution NMR and MRI with laser-polarized xenon. Science 271, 1848–1851.

(100). Stevens TK, Ramirez RM, and Pines A (2013) Nanoemulsion contrast agents with sub-picomolar sensitivity for xenon NMR. J. Am. Chem. Soc 135, 9576–9579. [PubMed: 23742228]

(101). Brotin T, and Dutasta JP (2009) Cryptophanes and their complexes—present and future. Chem. Rev 109, 88–130. [PubMed: 19086781]

(102). Kunth M, Dopfert J, Witte C, Rossella F, and Schroder L (2012) Optimized use of reversible binding for fast and selective NMR localization of caged xenon. Angew. Chem., Int. Ed 51, 8217–8220.

(103). Klippel S, Dopfert J, Jayapaul J, Kunth M, Rossella F, Schnurr M, Witte C, Freund C, and Schroder L (2014) Cell tracking with caged xenon: using cryptophanes as MRI reporters upon cellular internalization. Angew. Chem., Int. Ed 53, 493–496.

(104). Rose HM, Witte C, Rossella F, Klippel S, Freund C, and Schroder L (2014) Development of an antibody-based, modular biosensor for ^{129}Xe NMR molecular imaging of cells at nanomolar concentrations. Proc. Natl. Acad. Sci. U.S.A 111, 11697–11702. [PubMed: 25071165]

(105). Klippel S, Freund C, and Schroder L (2014) Multichannel MRI labeling of mammalian cells by switchable nanocarriers for hyperpolarized xenon. Nano Lett. 14, 5721–5726. [PubMed: 25247378]

(106). Shapiro MG, Ramirez RM, Sperling LJ, Sun G, Sun J, Pines A, Schaffer DV, and Bajaj VS (2014) Genetically encoded reporters for hyperpolarized xenon magnetic resonance imaging. Nat. Chem 6, 629–634. [PubMed: 24950334]

(107). Yang X, Song X, Li Y, Liu G, Ray Banerjee S, Pomper MG, and McMahon MT (2013) Salicylic acid and analogues as diaCEST MRI contrast agents with highly shifted exchangeable proton frequencies. Angew. Chem., Int. Ed 52, 8116–8119.

(108). Sun PZ, Benner T, Kumar A, and Sorensen AG (2008) Investigation of optimizing and translating pH-sensitive pulsed-chemical exchange saturation transfer (CEST) imaging to a 3T clinical scanner. Magn. Reson. Med 60, 834–841. [PubMed: 18816867]

(109). Smith SA, Farrell JA, Jones CK, Reich DS, Calabresi PA, and van Zijl PC (2006) Pulsed magnetization transfer imaging with body coil transmission at 3 T: feasibility and application. Magn. Reson. Med 56, 866–875. [PubMed: 16964602]

(110). Soesbe TC, Ratnakar SJ, Milne M, Zhang S, Do QN, Kovacs Z, and Sherry AD (2014) Maximizing T2-exchange in Dy3+DOTA-(amide) chelates: fine-tuning the water molecule exchange rate for enhanced T2 contrast in MRI. Magn. Reson. Med 71, 1179–1185. [PubMed: 24390729]

(111). Li AX, Hudson RH, Barrett JW, Jones CK, Pasternak SH, and Bartha R (2008) Four-pool modeling of proton exchange processes in biological systems in the presence of MRI-paramagnetic chemical exchange saturation transfer (PARACEST) agents. Magn. Reson. Med 60, 1197–1206. [PubMed: 18958857]

(112). Kim M, Gillen J, Landman BA, Zhou J, and van Zijl PC (2009) Water saturation shift referencing (WASSR) for chemical exchange saturation transfer (CEST) experiments. Magn. Reson. Med 61, 1441–1450. [PubMed: 19358232]

(113). Singh A, Cai K, Haris M, Hariharan H, and Reddy R (2013) On B1 inhomogeneity correction of in vivo human brain glutamate chemical exchange saturation transfer contrast at 7T. Magn. Reson. Med 69, 818–824. [PubMed: 22511396]

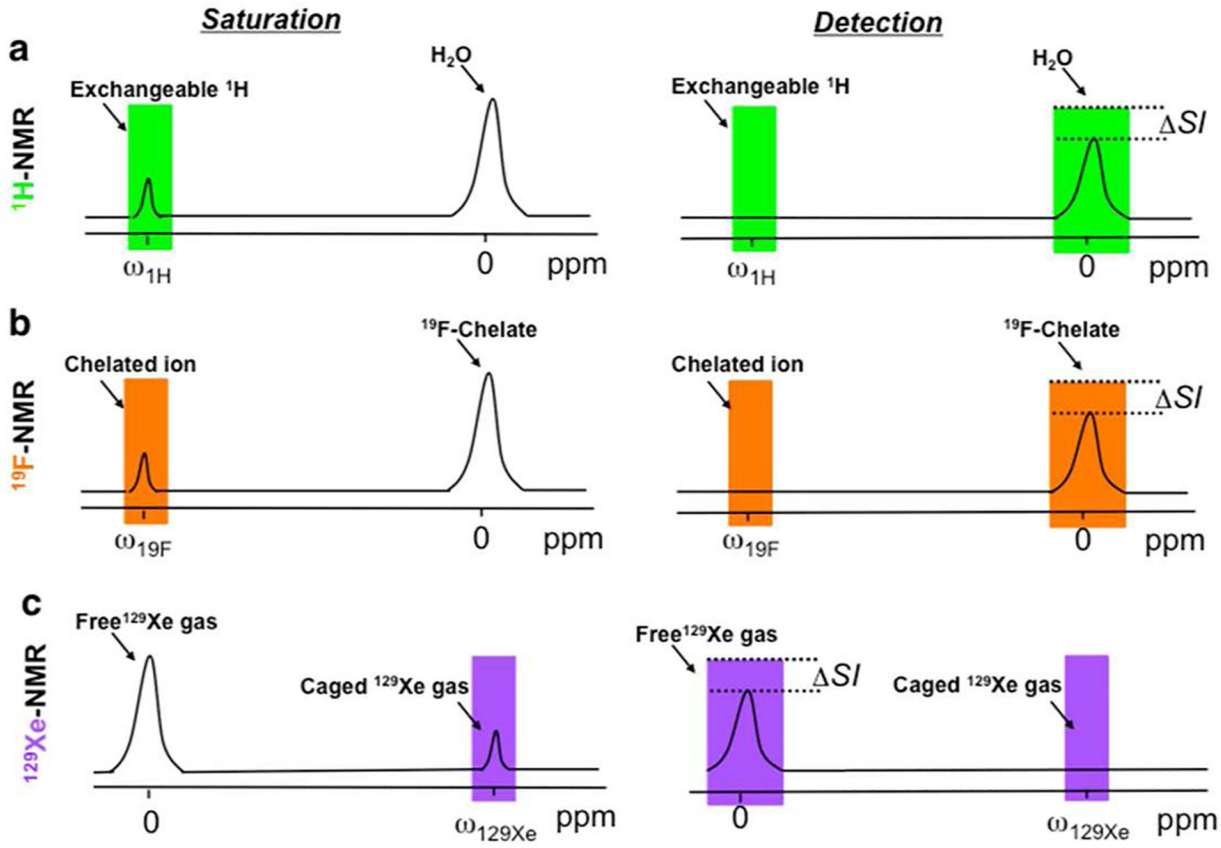

Figure 1.

Principles of CEST MRI. A frequency-selective saturation pulse (saturation) is applied to label exchangeable protons (a) or molecules (b, c) to achieve a reduction in the bulk signal (ΔSI, change in signal intensity) from the chemical exchange process (detection). Shown are current examples for ^1H_2O (a), a ^{19}F chelate (b), and ^{129}Xe gas (c).

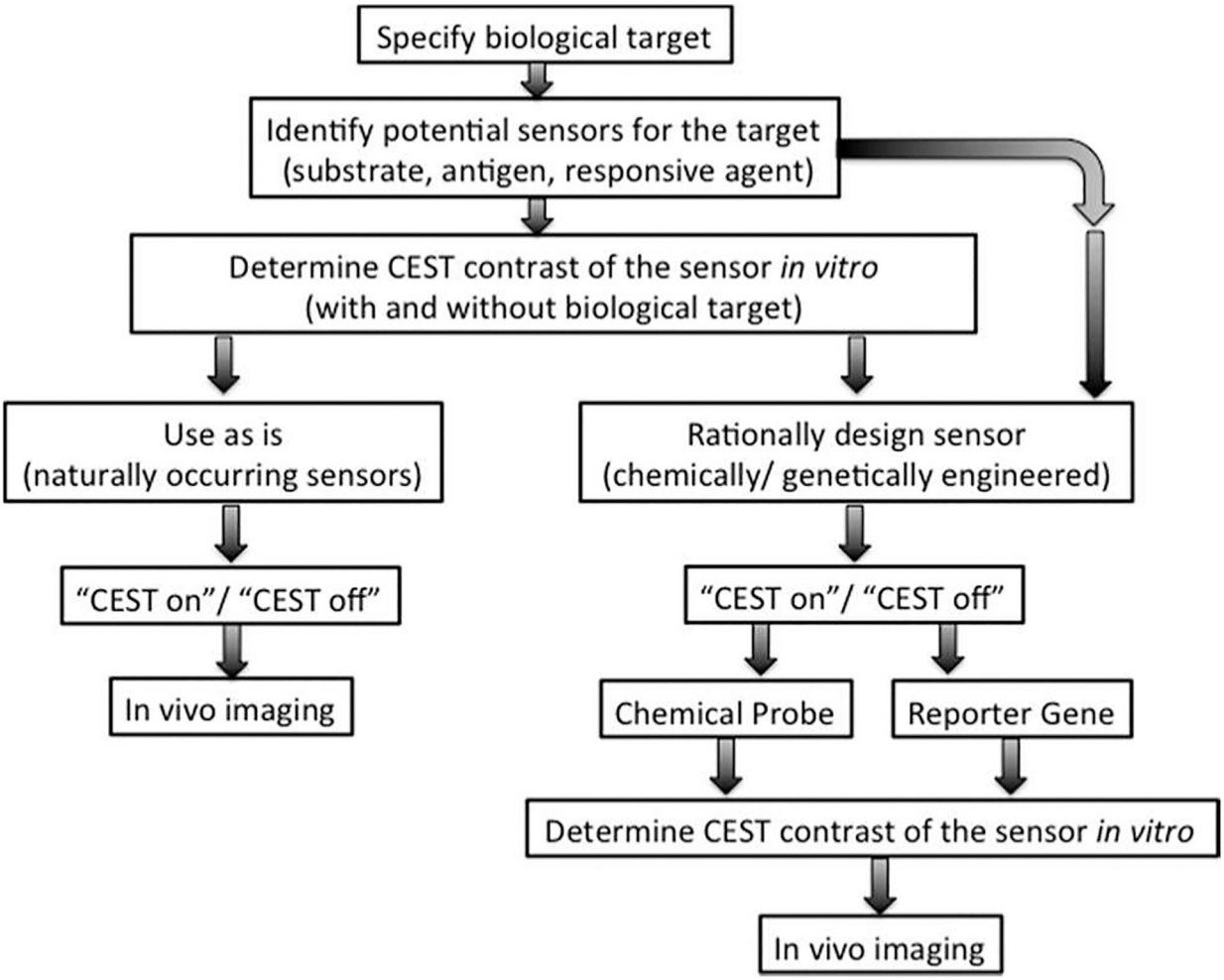

Figure 2.
Rational design of developing a CEST biosensor.

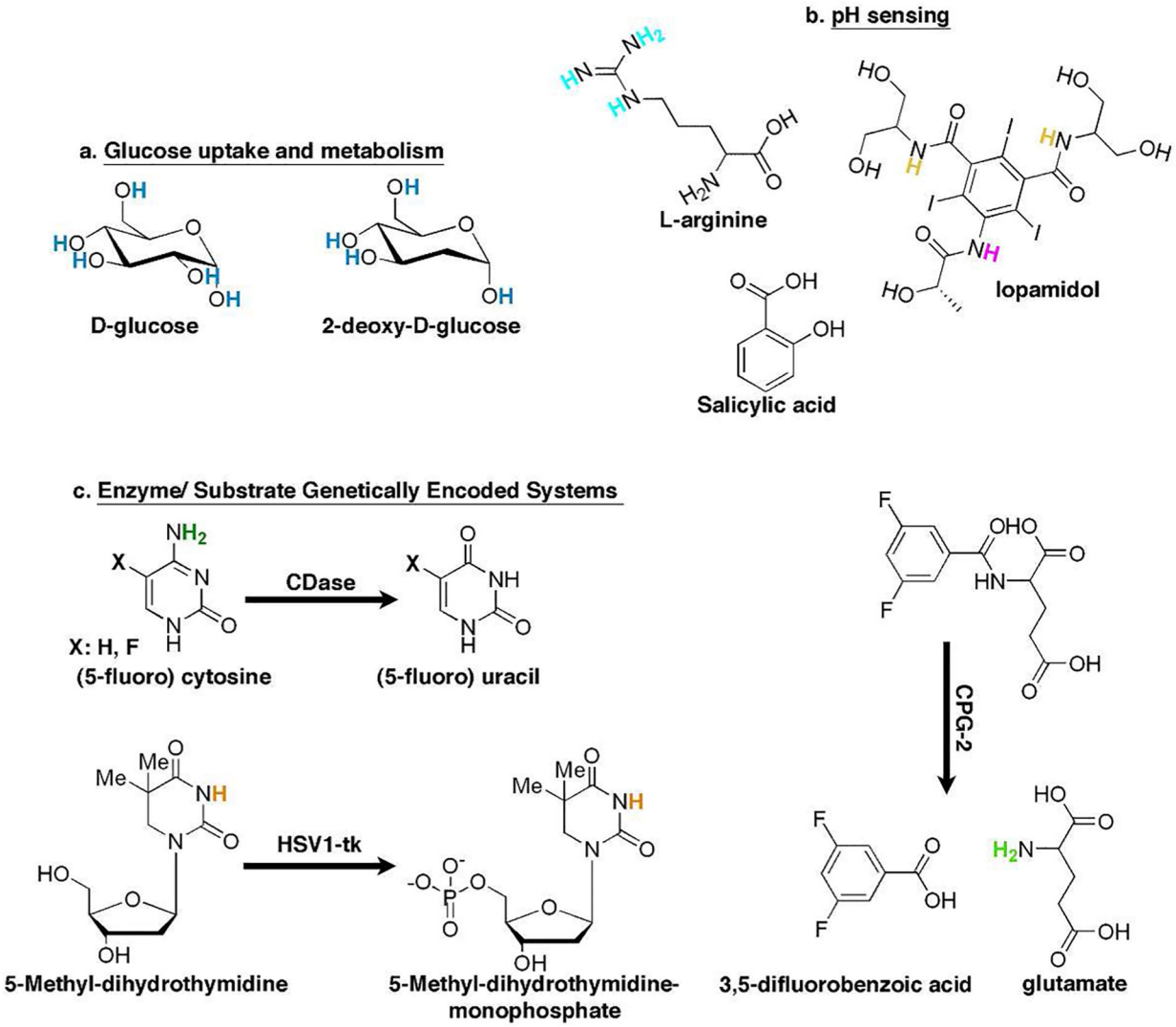

Figure 3.

Small molecules as CEST biosensors. The chemical structure of small molecules (natural or synthetic) that are being used as CEST sensors for monitoring: glucose uptake (a) and metabolism, pH (b), and genetically encoded enzyme/substrate systems (c).

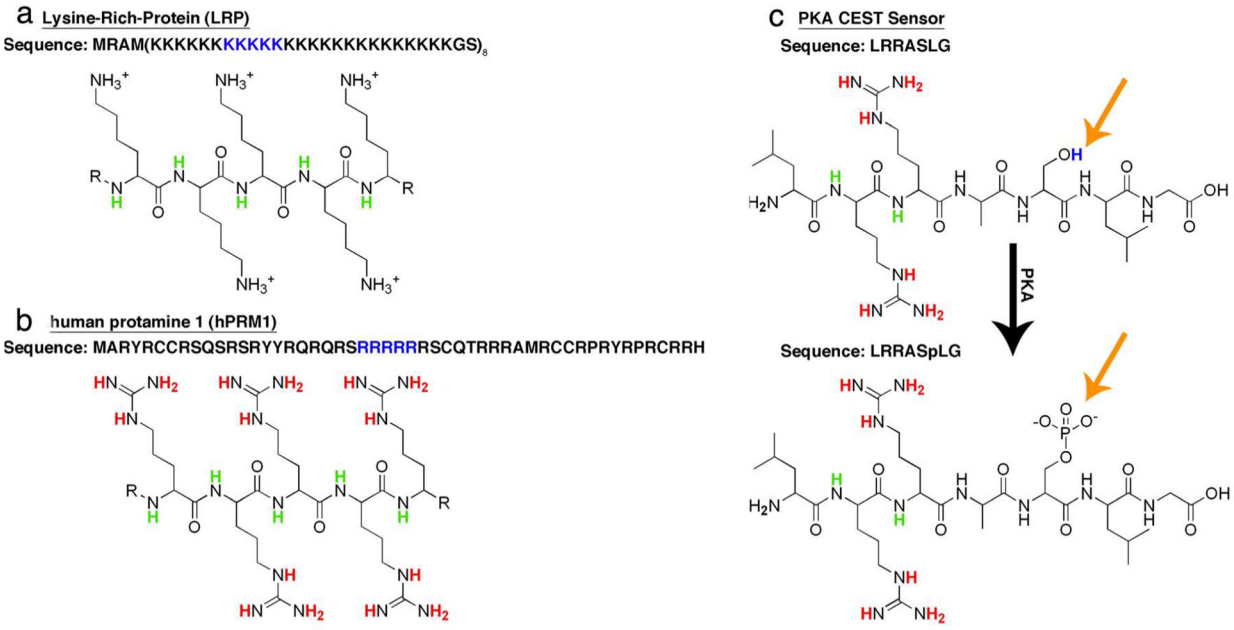

Figure 4.

CEST reporter genes. CEST reporter gene genes based on artificial (LRP) (a) and human (hPRM1) (b) proteins. (c) Genetically engineered responsive CEST reporter gene designed to image PKA activity. The full sequence of the protein is given by the single-letter amino acid code (i.e., K for lysine, R for arginine, and S for serine). The chemical structure of part of the sequence is presented.

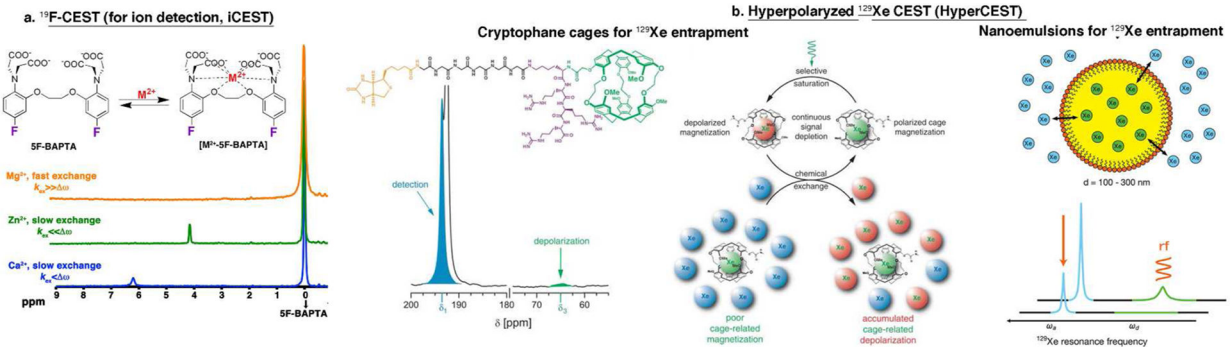

Figure 5.

Heteronuclear CEST (HeteroCEST) sensors. (a) Schematic depiction of the dynamic exchange process between free 5F-BAPTA and M^{2+}-bound [M^{2+}-5F-BAPTA] and the obtained ^{19}F NMR spectra of 5F-BAPTA in the presence of different M^{2+} ions. (b) Two suggested systems for HyperCEST. (i, left and middle panels) Cryptophane cage-based system: The chemical structure of the Xe biosensor illustrating the cryptophane-A cage (green), the linker (black), and the targeting moiety (biotin in this case, orange) and the ^{129}Xe-NMR spectrum of free and caged Xe gas. The middle panel shows a schematic illustration of the HyperCEST concept. (ii, right panel) Schematic illustration of Xe atoms that exchange between the interior of the nanoemulsion droplets and the bulk aqueous pool, which leads to two unique peaks in the ^{129}Xe spectrum. Adapted from refs 15 and 100. Copyright 2013 American Chemical Society. Adapted with permission from ref 16. Copyright 2006 American Association for the Advancement of Science.